FYS3150

PHASE TRANSITIONS OF 2D ISING MODEL

November 21, 2018

By Steinn Hauser Magnússon
Univerity of Oslo, UiO
Computational Physics Project 4

Abstract

A study regarding the simulation of a lattice consisting of spin-up and spin-down atoms is presented. The Ising model and Monte-Carlo method are the basis for the material's energy model and simulation. The Metropolis algorithm (a Markov Chain Monte Carlo method) was used to simulate probabilistic behaviour of the lattice using the Boltzmann distribution. The *ran2* RNG was used to simulate random characteristics of the system such as energy, magnetization, heat capacity and magnetic susceptibility. These were used to study several cases with different objectives regarding the observable lattice parameters. Finally, an extraction of the critical temperature in the thermodynamic limit (lattice size $L \to \infty$) is performed on larger simulations. C++ code was parallelized for optimization and the critical temperature was found to be $T = 2.267 \pm 0.006 kT_C J^{-1}$.

Contents

INTRODUCTION

Many-particle system simulation is a complex theme of modern science as there is great balance to be found therein. On one hand, the accuracy of the simulation should be maximized to consistency with reality, yet on the other there is a need for simplicity. Simulating systems brings a certain yearn of computational efficiency and performance. One seeks simplified models to summarize and clarify the complexity which arises from certain many-body systems. This is especially relevant in the case of interacting particle systems, as the current theory of quantum mechanics dictates that all the particles interact with each other in a fashion which is neither intuitive nor concise. This research will seek to simplify the model of a lattice of spin-up and down atoms to be fit for simulation on a large scale. The simulation is designed to calculate a number of characteristic physical properties about the system such as the magnetization, energy, heat capacity and magnetic susceptibility. A thermodynamic distribution model is introduced, and the system is simulated and analyzed for several different temperatures. This report is designed to brief the reader on the theoretical background required for the analyses, before explaining in detail the research methods and their objectives. The results are then presented and followed by an appropriate discussion and interpretation of the data. Finally, a fitting conclusion of the research project is stated to summarize.

The project covers multiple areas of research involving comparison and analyses of numerical results. These involve simulation of a 2×2 lattice, simulation and steady-state analyses of a 20×20 lattice for two temperatures $T = 1.0$ and $T = 2.4$, analyses of the probability distribution of these states, and finally a study of phase transitions exhibited by the lattice. The **Method**, **Results** and **Discussion** sections are therefore divided into subsections going into detail on the various areas of research. The research subsections are presented as:

- Two by two lattice
- Equilibrium time of larger lattice
- Energy distribution analysis
- Phase transition of lattices

The simulation method presented in the research was a script built in C++ and plotted in Python. This was a collaborative effort between Steinn Hauser and Simen Håpnes, and the program can be found on the following public GitHub repository:
`https://github.com/steinnhauser/FYS3150`

THEORY

Consider a lattice structure in two dimensions filled with atoms, each atom existing in one of two discrete states: Spin up or Spin down. This spin is an intrinsic characteristic of the atom which produces a small magnetic moment μ in the direction of the spin. The spin of an atom can therefore be flipped if influenced by a sufficiently powerful outer magnetic field. This means that if 90% of all lattice spins are pointing in the same direction, the sum of the magnetic moments produce a strong field which will likely cause the rest to follow. This is the case for materials such as iron where all the atomic spins are oriented in the same direction, resulting in a permanently magnetic material. This is categorized as a ferromagnetic material, and produces a magnetic field without the need of an outer influence. Iron is a typically ferromagnetic material as we experience it at room temperature, but this is not always the case if the material is heated.

Curie Temperature

The Curie temperature is a characteristic temperature of a material, varying depending on the material's particle size, the environmental pressure, material composition etc. This temperature is defined as the point at which a material's magnetization transitions from being permanent to having spin-dipoles which don't align with each other. The material then loses its net magnetization as the magnetic moments of the atoms cancel each other out. This is a spontaneous process which occurs due to a combination of multiple complex factors, causing ferromagnetic materials (intrinsically magnetic) to exhibit paramagnetic conduct. Paramagnetization is a phenomena in which a material has a disordered atomic-spin orientation in the absence of an outer magnetic field influence. This implies that the material has zero net magnetization. There are several models for calculating the Curie temperature for a material analytically, though the problem is far more suitable for numerical simulation and data analysis.

Mean-field theory and the Ising model

The mean-field theory is a theoretical model which works to simplify the behaviour of a large number of interacting components; this is highly applicable to the large number of discrete atomic spins system at hand. In reality, the interplay between all the atoms is an incredibly complex system of particle interaction, though the mean-field theory studies these effects in a simplified fashion. To implement the mean-field theory to the research at hand, the *Ising model* is presented. The Ising model involves assuming that each particle only interacts with it's nearest neighbours in a material lattice. This is a simplification of the complexities of reality but is certainly appropriate to a numerical simulation model, as the atoms have discrete up- and down-spins which the Ising model is applicable to. If each atom's spin in the lattice only interacts with its nearest neighbor, then the number of factors to be taken into consideration is significantly decreased, and the system can be

simulated efficiently. In the Ising model, the force of interaction between bodies is expressed by a weight J, which is used to indicate the strength of the potential between particles. This parameter is called the coupling constant, and varies depending on the system. It is used to approximate the effect sum of multiple particles to a single averaged coupling effect with its nearest neighbors. Assuming that the particles only interact with their nearest neighbors (weighted with a parameter J) produces the following expression for the energy of any particle in the lattice:

$$E = -J \sum_{\langle kl \rangle} s_k s_l \tag{1}$$

This is the energy expression of the Ising model which is used for the research at hand. s_k and s_l are the spins of the particles ($s \in \{-1, +1\}$) and the indexing $\langle kl \rangle$ symbolizes the nearest neighbors of the particle. I.e., for a square lattice of size $L \times L$ (L is a positive integer), where particles can have coordinates in the grid (x_i, y_i) ($x_i \wedge y_i \in [1, L]$), the nearest neighbors of the particle are then given by the four particles with coordinates $(x_{i\pm1}, y_{i\pm1})$. It is worth noting that when calculating the total energy of a lattice this way, it is important to count the energy contribution between two atoms only once. It is also worth noting that if all atoms were to be pointing in the same direction, the energy level per atom will be equal to $-2J$ by this model, regardless of lattice size.

This expression for the energy assumes that there are no external magnetic or electric fields which influence the particles of the system. In this research, a *periodic boundary condition* will be implemented in the edge points of the lattice to avoid discontinuity. This involves binding the outer lattice points together such that the nearest neighbors of, for example the edge $(1, 1)$, has energy contributions from the particle at the opposite edge (L, L). This is analogous to connecting the square lattice to form a torus.

Monte-Carlo method, Markov-Chains and Random numbers

Simulating the lattice will involve a combination of interconnected algorithm methods, but the leading component of simulation is the Monte-Carlo method. This method is implemented to simulate the lattice in a probabilistic manner using a probability distribution function (PDF) and sampling rule. The sampling rule dictates whether a probabilistic event occurs depending on a random number generator (RNG). This sampling rule combined with the RNG makes certain that an event which has an 80% chance of occurring, actually follows that probabilistic pattern. The sampling rule will be gone into greater detail in the **Metropolis algorithm** section.

The Metropolis algorithm is a Markov-chain Monte Carlo (MCMC) method, where Markov-chains are used to simulate probabilistic changes. To describe Markov-chains, consider a system with two states j and i, where

the probability of transitioning from state j to i is given by:

$$P_j = T_{j,i} A_{j,i}. \tag{2}$$

$T_{j,i}$ is the probability of the transition from state j to i occurring, and $A_{j,i}$ is the probability describing whether or not that transition should occur. It can be shown that the following is also valid [2]:

$$P_j T_{j,i} A_{j,i} = P_i T_{i,j} A_{i,j}, \tag{3}$$

where the T probabilities are assumed to be equal. From this, the probability of the new state i being chosen is given by:

$$A_{j,i} = min\left\{1, \frac{P_i}{P_j}\right\}. \tag{4}$$

This is the essence of the Markov-Chain. Note that if the probability of the new state $P_i > P_j$, the transition probability from j to i is 1 (or 100%). Otherwise, the probability ratio is evaluated in relation to a random number generator. This also will be gone into greater detail in the **Metropolis algorithm** section.

In order to generate random number values for the code, a random number generator algorithm known as *rand2* is used[5]. This algorithm has a period $\approx 2.3 \cdot 10^{18}$ (takes a long time before it repeats itself) and has withstood several RNG tests which confirm its eligibility (though it has twice the execution time of *rand0* and $\approx 1.54\times$ the execution time of *rand1* [4]). The algorithm takes in a negative integer seed which produces the first random value between 0 and 1. The seed value is changed in this process and is cycled back into the RNG for the next value.

The numbers generated by this function are of course pseudo-random, meaning that they are not truly random but rather have random-looking tendencies. These values are predictable if the seed is known, so a new seed is used each time a simulation is run in the lattice program. Precisely this is done to calculate the mean values of the system, as using only one run may produce results which are characteristic to the input seed. The average of ten different runs (using ten different seeds) is typically sufficient to calculate the average values of the lattice numerically for comparison with analytic values.

Expectation values

The analytic expectation value expression of a general observable parameter x is given by the following relation [6]:

$$\langle x \rangle = \frac{1}{Z} \sum_S x e^{-\beta E_S} \tag{5}$$

Z is the partition function which corresponds to the system's current temperature, and $e^{-\beta E_S}$ is the Boltzmann factor for the energy state E_S. The factor β is given by $\beta = 1/(k_B T)$, where k_B is Boltzmann's constant and T is the temperature in kelvin. This general expression allows for the calculation of the expectation values of the parameters $\langle E \rangle$, $\langle E^2 \rangle$, $\langle |M| \rangle$ and $\langle M^2 \rangle$ for later comparison of the numerical values for a 2×2 lattice. Table 1 lists all possible configurations of the lattice (as a function of the number of spin-up atoms # $\uparrow$), as well as the degeneracy (number of states with the same energy) of the energy state:

# $\uparrow$	Degeneracy #	Energy E	Magnetization M
4	1	$-8J$	4μ
3	4	0	2μ
2	4	0	0
2	2	$8J$	0
1	4	0	-2μ
0	1	$-8J$	-4μ

Table 1: Table of the values of the energy and magnetization for every spin-up configuration of a two times two lattice. The energies are calculated by hand using periodic boundary conditions and equation 1.

These are the energy values which are used in the Boltzmann factor expressed in equation 5. The partition function Z (normalization constant of the probabilities) is given by

$$Z(\beta) = \sum_S e^{-\beta E_S}, \tag{6}$$

where S expresses all the possible states the system has access to. Inserting the values from table 1 produces the following partition function for the 2×2 lattice:

$$Z(\beta) = e^{-\beta(-8J)} + 4 + 4 + 2e^{-\beta 8J} + 4 + e^{-\beta(-8J)} = 12 + 2e^{\beta 8J} + 2e^{-\beta 8J} \tag{7}$$

The coefficients of the expression are a result of the degeneracy states described in table 1. This can be simplified by the hyperbolic cosine function identity $cosh(x) = (e^x + e^{-x})/2$:

$$Z(\beta) = 12 + 4\cosh(\beta 8J) \tag{8}$$

This partition function is now used to calculate the expectation values using equation 5, beginning with $\langle E \rangle$:

$$\langle E \rangle = \frac{1}{12 + 4\cosh(\beta 8J)} \sum_{i=1}^{16} E_i e^{-\beta E_i} \tag{9}$$

$$\Rightarrow \langle E \rangle = \frac{16Je^{-\beta 8J} - 16Je^{\beta 8J}}{12 + 4\cosh(\beta 8J)} \tag{10}$$

The trigonometrical identity for the hyperbolic sine function $\sinh(x) = (e^x - e^{-x})/2$ returns the expectation value of the energy to be:

$$\langle E \rangle = \frac{32J\sinh(-\beta 8J)}{12 + 4\cosh(\beta 8J)} \Rightarrow \langle E \rangle = \frac{8J\sinh(-\beta 8J)}{3 + \cosh(\beta 8J)} \tag{11}$$

Following are the expressions for $\langle E^2 \rangle$, $\langle |M| \rangle$, $\langle M^2 \rangle$ derived in the same fashion:

$$\langle E^2 \rangle = \frac{1}{12 + 4\cosh(\beta 8J)} \sum_{i=1}^{16} E_i^2 e^{-\beta E_i^2} \tag{12}$$

$$\langle E^2 \rangle = \frac{256J^2\cosh(\beta 8J)}{12 + 4\cosh(\beta 8J)} \tag{13}$$

$$\Rightarrow \langle E^2 \rangle = \frac{64J^2\cosh(\beta 8J)}{3 + \cosh(\beta 8J)} \tag{14}$$

$$\langle |M| \rangle = \frac{1}{12 + 4\cosh(\beta 8J)} \sum_{i=1}^{16} |M_i| e^{-\beta E_i^2} \tag{15}$$

$$\langle |M| \rangle = \frac{8e^{\beta 8J} + 4}{12 + 4\cosh(\beta 8J)} \tag{16}$$

$$\Rightarrow \langle |M| \rangle = \frac{2e^{\beta 8J} + 1}{3 + \cosh(\beta 8J)} \tag{17}$$

$$\langle M^2 \rangle = \frac{1}{12 + 4\cosh(\beta 8J)} \sum_{i=1}^{16} M_i^2 e^{-\beta E_i} \tag{18}$$

$$\langle M^2 \rangle = \frac{32e^{\beta 8J} + 8}{12 + 4\cosh(\beta 8J)} \tag{19}$$

$$\Rightarrow \langle M^2 \rangle = \frac{8e^{\beta 8J} + 2}{3 + \cosh(\beta 8J)} \tag{20}$$

The specific isocoric (fixed volume V) heat capacity C_V and the magnetic susceptibility χ can now be calculated

analytically, since the two are then given by [2]:

$$C_V = \frac{1}{kT^2}\sigma_E^2 \tag{21}$$

$$C_V = \frac{1}{kT^2}\left(\langle E^2\rangle - \langle E\rangle^2\right) \tag{22}$$

$$C_V = \frac{1}{kT^2}\left[\frac{64\cosh(\beta 8J)}{3+\cosh(\beta 8J)} - \left(\frac{8\sinh(-\beta 8J)}{3+\cosh(\beta 8J)}\right)^2\right] \tag{23}$$

$$\chi = \frac{1}{kT}\sigma_M^2 \tag{24}$$

$$\chi = \frac{1}{kT}\left(\langle M^2\rangle - \langle |M|\rangle^2\right) \tag{25}$$

$$\chi = \frac{1}{kT}\left[\frac{8e^{\beta 8J}+2}{3+\cosh(\beta 8J)} - \left(\frac{2e^{\beta 8J}+1}{3+\cosh(\beta 8J)}\right)^2\right] \tag{26}$$

The research will be scaled such that $J = k = 1$. This means that the temperature has units of energy and that the parameters are given in terms of Boltzmann's constant k. This is done to express the parameters in values which are more applicable numerically, as a value which is too small or large can quickly result in numerical errors (underflow, overflow, round-off, etc.).

These parameters are linked to a system's thermodynamic quantity F, formally referred to as the Helmholtz' free energy:

$$F = U - TS \tag{27}$$

U is the internal energy of the system, T is the absolute temperature and S is the system's final entropy. In the case of the Ising model, both the heat capacity C_V and magnetic susceptibility χ are second derivatives of the Helmholtz' free energy F. This implicates that C_V and χ are both discontinuous at the critical temperature T_C described previously [2]. The Ising model therefore exhibits a second order phase transition (in the thermodynamic limit $L \to \infty$) at the critical temperature which can be seen by observation of the parameters C_V and χ in the domain around T_C. To calculate the critical temperature T_C numerically, the correlation length ξ is introduced:

$$\xi(T) \sim |T_C - T|^{-\nu} \sim L \tag{28}$$

ν is a constant, and T_C is the critical temperature. Since the correlation length is proportional to L, the relation can be rewritten as the following:

$$T_C(L) - T_C(L=\infty) = aL^{-1/\nu} \tag{29}$$

a is a constant, and the case of $\nu = 1$ will be studied further. Rewriting this equation by introduction of two

lattice sizes L_1 and L_2 (and acknowledging that a is the same for all lattice sizes) allows us to extract a value for $T_C(L=\infty)$:

$$T_C(L_1) - T_C(\infty) = \frac{a_1}{L_1} \tag{30}$$

$$a_1 = L_1(T_C(L_1) - T_C(\infty)) \tag{31}$$

Inserting this in for another lattice size L_2 and solving for $T_C(L=\infty)$ produces the following relation:

$$T_C(L_2) - T_C(\infty) = \frac{a_1}{L_2} \tag{32}$$

$$T_C(L_2) - T_C(\infty) = \frac{L_1(T_C(L_1) - T_C(\infty))}{L_2} \tag{33}$$

$$\Rightarrow T_C(\infty) = \frac{L_2 T_C(L_2) - L_1 T_C(L_1)}{L_2 - L_1} \tag{34}$$

This is the equation used to extract the critical temperature from the simulation study.

Metropolis algorithm

The Metropolis algorithm is the component of the script in determining the evolution of the lattice. This algorithm is a special case combination of *Markov chains* and the *Monte Carlo method* (MCMC method), where an input PDF is utilized to generate probabilististic sequences of events. For utilization of Markov chains, however, two principal conditions must be satisfied: *Ergodicity* and *Detailed balance*.

Ergodicity means that it is possible to access all possible states. This principal is fulfilled by the Boltzmann factor presented previously, which states that any particle flip has a non-zero probability of occurring, regardless of its surroundings. This entails that any $2^{L\times L}$ lattice spin configuration is theoretically possible, though some are certainly more probable than others. Detailed balance indicates that a steady-state solution to a process is non-cyclic. In other words, the configuration of a state in the limit of time $t \to \infty$ has only one solution. Some systems can exhibit cyclic steady-state processes, where two or more states are equally probable in the time limit. The Ising model simulation does not exhibit cyclic steady-state solutions due to *reversibility* [1].

The Metropolis algorithm with the Boltzmann factor applied to the Ising model therefore fulfills *ergodicity* and *detailed balance*. Further, the Metropolis algorithm evaluates the ratio between two probabilistic occurrences and dictates which of these should happen through random number generation:

$$r \leq \frac{P_j}{P_i} \tag{35}$$

The randomly generated number r is within the domain $r \in [0,1]$ (found using the uniform distribution RNG *ran2* described previously) dictates whether the candidate state with probability P_j is preferable to the initial state P_i. In the case $P_j \geq P_i$, the new state j is always accepted. The case of $P_j < P_i$ is determined by the random number r. The probability distribution model P used for the lattice research is the Boltzmann factor combined with the partition function

$$P_s = \frac{1}{Z} e^{-\beta E_s} \tag{36}$$

described previously. The ratio between two such factors dictates the likelyhood of a state with energy E_i being changed to the state E_j, and the Metropolis algorithm is then applied to assess whether or not this change in energy should occur. Additionally, this model carries an excellent numerical practicality in that the partition function Z is irrelevant to the probability ratio calculation:

$$r \leq \frac{e^{-\beta E_j}/Z}{e^{-\beta E_i}/Z} \tag{37}$$

$$r \leq e^{-\beta \Delta E}. \tag{38}$$

$\Delta E = E_j - E_i$ is the change in energy of the initial state and the candidate state proposed. Recalling the principle of minimal energy, which states that a system always prefers the state of least energy, the state $E_j < E_i \leftrightarrow \Delta E < 0$ is the most likely to occur over time. These are the determining factors of the simulation at hand.

METHOD

A lattice generator function was designed in the C++ script to take in several inputs depending on what kind of research is desired. It was initialized with inputs stating its size L (signifying an $L \times L$ lattice) and a variable which states whether or not the initial state is *ordered* or *disordered*. In the ordered case, all spins were set to $+1$, and in the disordered state, they were set to ± 1 randomly using the *ran2* RNG.

A temperature was then set (depending on the objective) to calculate the energy change exponentials (right side of equation 38) of the system. These were sometimes dependant on the size of the lattice (in the case of 2×2, the only energy changes possible are $[-8J, 0, +8J]$), but for larger lattices this change can be any of the following: $\Delta E \in [-8J, -4J, 0, +4J, +8J]$. These exponentials $e^{-\beta \Delta E}$ were therefore calculated into an array ω a single time for use later in the metropolis algorithm. The algorithm utilizes this array in the condition of acceptance of a new state $r \leq \omega(\Delta E)$, where $\omega(\Delta E) = e^{-\beta \Delta E}$ is the probability ratio between states.

After these were initialized, the lattice was sent into the metropolis algorithm function for simulation. The metropolis algorithm picks out random x and y indices and assesses whether or not it should be flipped by the

condition $r \leq \omega(\Delta E)$. If the condition is true, the spin was flipped and the new lattice was saved. This was done $L \times L$ times on random atoms of the lattice, signifying that most atoms will likely be examined, yet there was a chance for some to be proposed more than once. After all $L \times L$ candidates were determined (accepted or rejected), one sweep of the lattice was complete. This process is then repeated over several Monte Carlo (MC) cycles. The number of MC cycles simulated depended on the objective of the simulation.

Most research was oriented towards recording the energy and magnetization change as a function of the MC cycles; if an atom is flipped, the energy change was calculated and the change in spin (net magnetization) was given by the expression $-2 \cdot s$, where s was the previous spin of the electron. This was done for each flip accepted out of the $L \times L$ candidates, and the energy and magnetization difference were added (or subtracted) to the total energy and magnetization of the lattice.

The total energy and magnetization of the lattice per MC cycle were saved using the *vector* package in C++. These vectors were written out into binary files (to minimize the run-time of the program) for plotting and post-analyses in Python. Any other parameters of interest in more specific research cases were also written to files in this fashion.

Two by two lattice

The specific method for finding the numerical values of $\langle E \rangle$, $\langle |M| \rangle$, C_V and χ for the 2×2 lattice was as follows:

- Initialize the lattice calculating its initial energy and magnetization.
- Calculate the total change in energy and magnetization for each MC cycle.
- Save the energy and magnetization values of the lattice for each MC cycle.
- Calculate the mean and standard deviation of these values after all cycles.

This was the general approach to calculating the mean energy and magnetization values of the lattice numerically. The mean energy and magnetization are compared to the analytic results acquired from the **Expectation values** section (equations 11, 14, 17 and 20). The standard deviations of the energy and magnetization were similarly used to calculate and compare C_V and χ with their analytic models (equations 23 and 26).

To research the number of MC cycles required for accurate results, ten simulations were run using different RNG seeds. The script averaged the result of several random value cycles to avoid biased results produced by a single seed. The research was conducted for several different numbers of MC cycles N_{MC}. The variants $N_{MC} \in [10, 10^3, 10^5, 10^7]$ were used to see how many were required to reach a sufficiently accurate numerical

result in relation to the analytic values.

Equilibrium time of larger lattice

To research the equilibrium time and behaviour of a larger lattice, four different cases are presented:

- Ordered lattice, temperature $T = 1.0$
- Ordered lattice, temperature $T = 2.4$
- Disordered lattice, temperature $T = 1.0$
- Disordered lattice, temperature $T = 2.4$

In all four cases, the total energy and magnetization, and the total number of accepted configurations (accepted being dictated by the condition $r \leq \omega(\Delta E)$) were counted and plotted as functions of the MC cycles. Another analysis went into detail on when the lattice reached it's equilibrium state. For a lattice with a disordered initial state, the lattice is extremely unlikely to initialize in equilibrium; several MC cycles were therefore required for this steady state to be reached.

Several variants of computing the equilibrium time numerically are available, and the method chosen for this case was to declare the equilibrium state once the energy per spin of the lattice reached $-2J$. This state represents the lowest possible energy state for any lattice, as the periodic boundary condition and equation 1 reveal. A general equilibrium time calculation function was therefore designed to extract the number of MC cycles S required to reach equilibrium for any lattice of size L and temperature T. This result was dependant on the RNG seed used, so the function also received this as an input. To research the distribution of these equilibrium times, a large number of S samples were generated by calling on the function 10^6 times using a different RNG seed each time. This research was done specifically for randomly initialized 20×20 lattices at temperatures $T = 1.0$. A specific S domain was defined ($S \in [0, 3000]$ in this case), and the frequencies of the equilibrium times in this domain were counted using 10^6 equilibrium time samples. The average equilibrium time was calculated as well, informing about the most frequent (most likely) equilibrium time as well as the mean.

Energy distribution analysis

To calculate the energy distribution for the four states described above (ordered, disordered, $T = 1.0$, and $T = 2.4$), the energy values of the steady state were cycled through and counted. 10^7 MC cycles were applied to the four cases, and the first 3% of the MC cycles were ignored to ensure that a steady state was reached. The

following 9,700,000 MC cycles counted the number of energy state appearances. This was done in the following fashion:

- Calculate the mean μ and standard deviation σ_E of the energy distribution.
- Generate parameters $E_{min} = \mu - 4\sigma_E$ and $E_{max} = \mu + 4\sigma_E$.
- Cycle through energies E_{min} to E_{max} with step size $4J$.
- Count the number of simulated states which correspond to each energy value.

This method was conducted for several different seeds to assess how many MC cycles were required to avoid contributions from the non-steady state configuration. Sampling after the first 300,000 MC cycles guarantees steady-state samples for a very large number of seeds.

Phase transition of lattices

For simulation of phase transitions, the algorithm was designed to handle the computation of larger lattices by parallelization. This was done using the Open MPI package (version 2.1.1) for C++ which is designed to utilize each CPU of a computer by assigning them different jobs. Each processor ran the simulation independent of the others, and the data produced was gathered by use of open MPI's *Reduce* function. This function allowed for the communication between the cores and for allocation of the data. The cases which this parallelized version of the code researched were for larger lattice sizes in the range of $L \in [40, 60, 80, 100, 120]$. The temperatures calculated were in the domain $T \in [2.0, 2.6]$ and had a higher resolution around the theoretical critical temperature (after Lars Onsager [3]) $T_c \approx 2.269$. To do this, a customizeable temperature vector which dictates the temperatures calculated was implemented.

An important factor to take into consideration is the data collection relevance of the lattice. When calculating the mean values, an equilibrium state is required or else the data will include the random initial state variables. The equilibrium time S was therefore cycled through first before moving on to the number of MC cycles N_{MC} (where data is recorded). This S loop was done for only the first temperature, allowing the same equilibrium state lattice to proceed to the next temperature after data collection. This was to avoid initializing the lattice and applying the Metropolis algorithm S times for every temperature. Following is the general method of the research in chronological order:

- Initialized the CPU cores and a seed which is different for each one.
- Each core was assigned a number of MC cycles given by N_{MC}/C, where C is the number of cores.
- Looped through all the lattice sizes L desired.

- Initialized the spin matrix in a disordered configuration.
- The Metropolis algorithm was applied to the lattice S times using the first temperature.
- Looped through the temperatures desired, calculating a new ω array each time.
- The Metropolis algorithm was applied N_{MC}/C times and began sampling data.
- The data was collected by the *reduce* MPI function and written to a file.

Although temperature changes will have an impact on the behaviour of the lattice, it is appropriate to use the same lattice throughout the simulation. This reduces the run-time of the simulation significantly, as generating a new lattice would demand another equilibrium time S simulation.

The goal was to numerically extract a numerical critical temperature from the data. This was done by extracting the temperatures which produce the maximum values of C_V and χ for each lattice. The critical temperature in the thermodynamic limit $L \to \infty$ was then calculated by equation 34 for all lattice combinations L_1 and L_2. After the critical temperatures in the thermodynamic limit were calculated for all lattice combinations, the mean and standard deviation (representing uncertainty) of these data were representative of the research results for $T_C(L = \infty)$. This was done independently for both C_V and χ.

RESULTS

Two by two lattice

Table 2 lists the analytic and numeric value calculations for a 2×2 lattice at a temperature $T = 1.0$. The numeric values were calculated by a 10^7 MC cycle simulation. Ten runs were conducted with different seeds to average the numeric values.

Value	Analytic	Numeric	Relative error [‰]
$\langle E \rangle [J]$	-7.9839	-7.9840	0.017
$\langle E^2 \rangle [J^2]$	63.8714	63.8723	0.014
$\langle \lvert M \rvert \rangle [\mu]$	3.9946	3.9947	0.020
$\langle M^2 \rangle [\mu^2]$	15.9732	15.9734	0.012
$C_V [J^2 k^{-1} T^{-2}]$	0.1283	0.1275	6.5491
$\chi [J^2 k^{-1} T^{-1}]$	0.0160	0.0159	4.3066

Table 2: Table comparing the 2×2 lattice analytic calculations to the numeric results for the temperature $T = 1.0$. The energy is given in units of the coupling constant J and the magnetizations are given in units of single atom magnetic moments μ. 10 runs were run to calculate the average values using 10^7 MC cycles. The errors are given in per mille ‰. The time it took to calculate these values was $37.2s$.

Table 3 lists the numeric accuracy in per mille for several numbers of MC cycles. Ten runs with different seeds were run for each value to calculate averages.

MC cycles	Relative errors [‰]						Runtime
	$\langle E \rangle$	$\langle E^2 \rangle$	$\langle \lvert M \rvert \rangle$	$\langle M^2 \rangle$	$C_v[J^2k^{-1}T^{-2}]$	$\chi[J^2k^{-1}T^{-1}]$	
10	188.37	188.37	128.82	158.59	58360	62000	$21\mu s$
10^3	3.3943	2.9966	2.1529	2.6795	1870.4	1630.5	$0.43ms$
10^5	0.027	0.026	0.008	0.023	17.002	16.620	$37.2ms$
10^7	0.017	0.014	0.020	0.012	6.5491	4.3066	$3.72s$

Table 3: Relative errors of the 2×2 lattice expectation values, heat capacity and magnetic susceptibilities for different numbers of MC cycles at temperature $T = 1.0$. The errors are relative to the analytic values listed in table 2 and listed in per mille ‰. These values were dictated by the average of ten runs using different seeds.

Equilibrium time of larger lattice

Figure 1 illustrates the equilibrium time distribution in the MC cycle domain around $[0, 1000]$. Equilibrium times of 10^6 sampled 20×20 lattices are calculated at $T = 1.0$ using different seeds. The domain calculated was $[0, 3000]$, so figure 2 is also included for the MC cycle domain around $[1900, 2700]$.

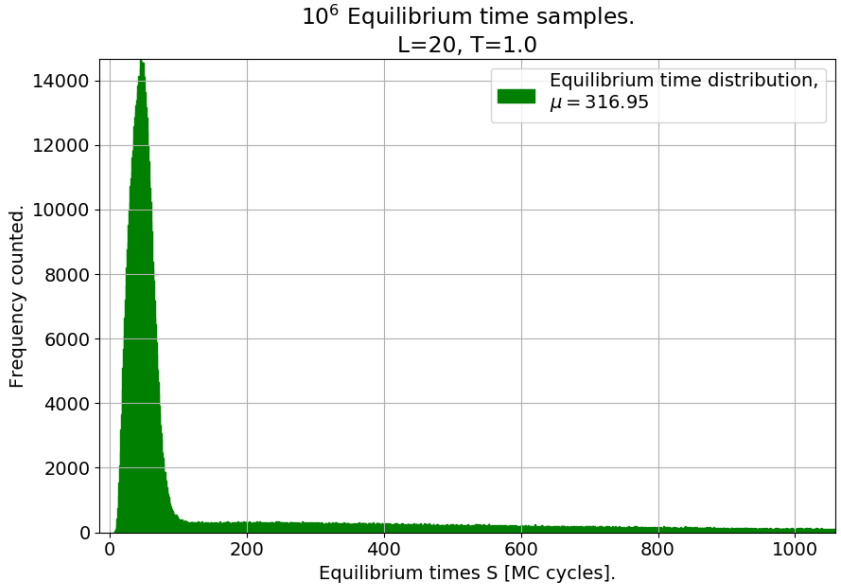

Figure 1: The total number of equilibrium times counted for 10^6 20×20 lattices at $T = 1.0$ with different seeds. The distribution conveys which equilibrium times are more frequent than others. The figure illustrates the distribution in the equilibrium time domain $S \in [0, 1000]$ MC cycles

Figure 2 illustrates the same equilibrium time S distribution as figure 1, though in the domain of $S \in [1900, 2700]$ MC cycles.

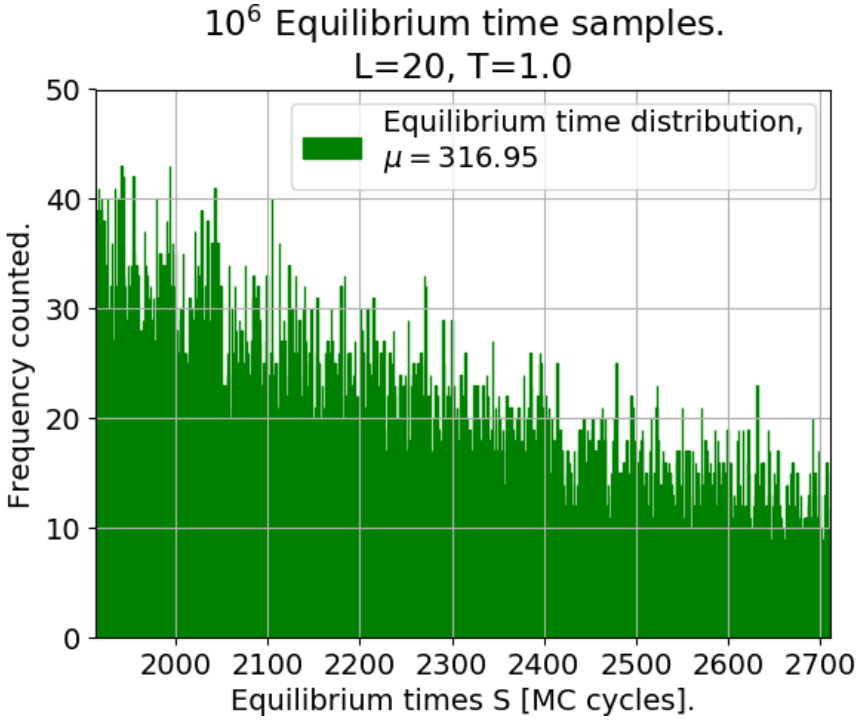

Figure 2: The total number of equilibrium times counted for 10^6 20×20 lattices at $T = 1.0$ with different seeds. The distribution conveys which equilibrium times are more frequent than others. The figure illustrates the distribution in the equilibrium time domain $S \in [1900, 2700]$ MC cycles.

Figure 3 illustrates the four simulated combinations of ordered and random initial conditions, and temperatures $T = 1.0$ and $T = 2.4$. The lattice size for all plots is 20×20 and the total simulation time is 10^4 MC cycles. Both the energy and magnetization graphs are scaled to illustrate the energy and net magnetization per spin atom.

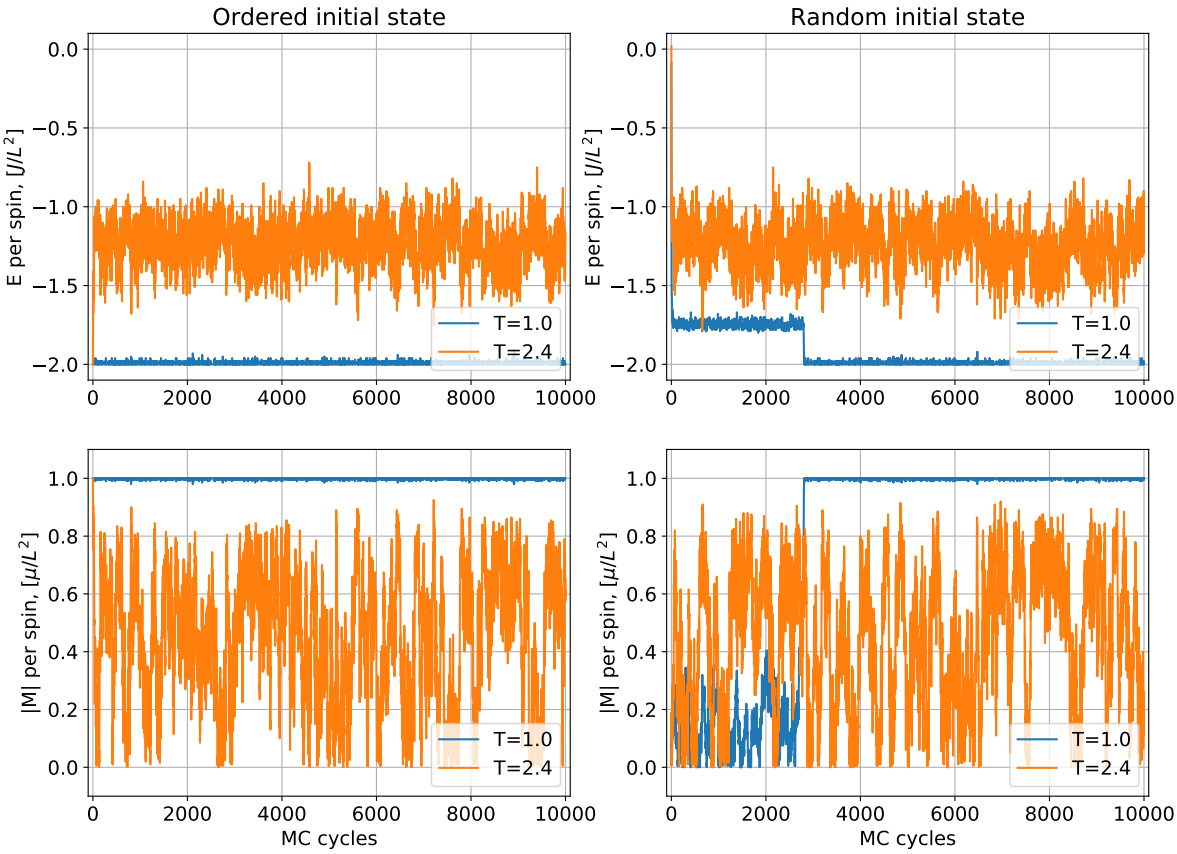

Figure 3: Mean energy and magnetization per spin for the four configurations (ordered, disordered, $T = 1.0$ and $T = 2.4$). All cases had a 20×20 lattice simulated for 10^4 MC cycles.

Figures 4 and 5 illustrate the total number of accepted configurations (accepted meaning that the condition in equation 38 is fulfilled) for the 20×20 lattice. Figure 4 is the plot of the total number of accepted configurations per MC cycle for the temperature $T = 1.0$. Figure 5 illustrates the total number of accepted configurations as a function of the temperature. Each point represents the total number of accepted configurations over 10^5 MC cycles.

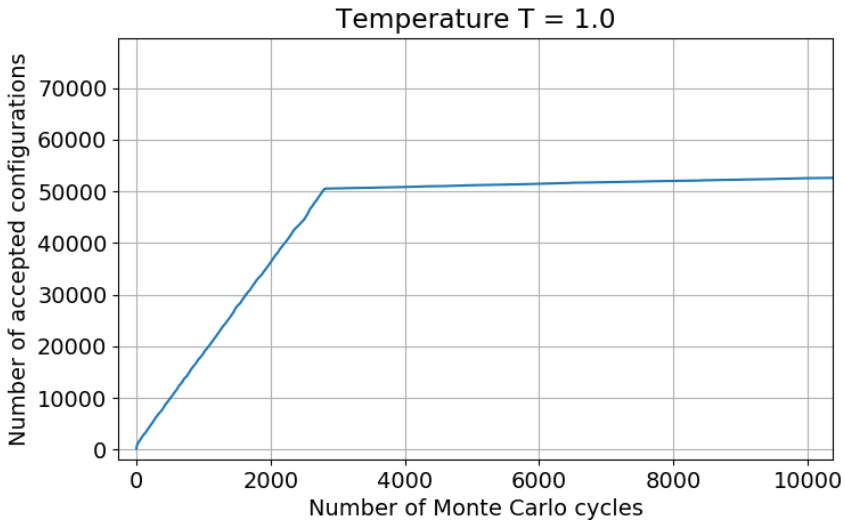

Figure 4: The number of total accepted configurations as a function of the MC cycles. The lattice size is 20×20 and the temperature is $T = 1.0$. An area of interest is illustrated, as the graph proceeded linearly from $MC \in [10^4, 10^5]$.

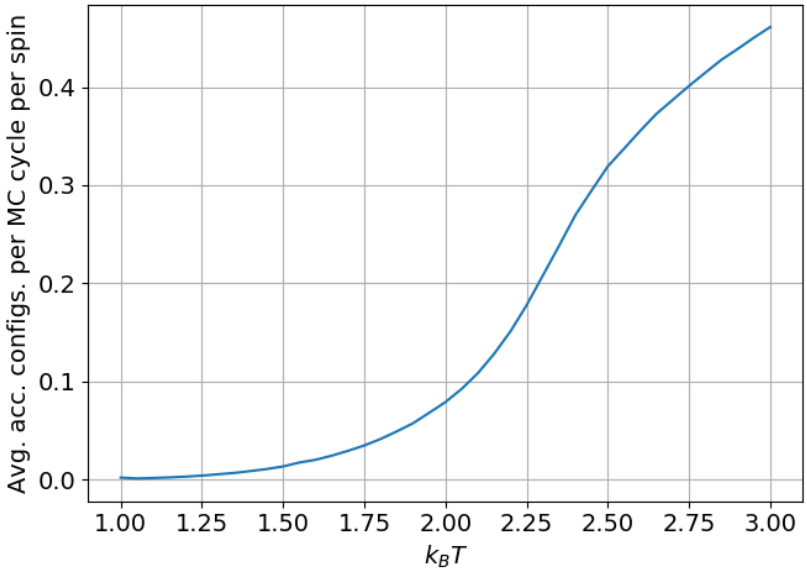

Figure 5: The average number of accepted configurations per MC cycle as a function of the temperature. The temperatures included are from $T = 1.0$ to $T = 3.0$ with step size $dT = 0.05$. The lattice size is 20×20 and the number of MC cycles used to calculate each data point is 10^5.

Energy distribution analysis

Figure 6 illustrates the four calculated probability distributions of the energy levels for the simulations of ordered and random initial conditions, and temperatures $T = 1.0$ and $T = 2.4$. All shared a lattice size of 20×20 and a simulation time of $9.7 \cdot 10^6$ MC cycles. The first 3% of the MC cycles were not recorded to ensure that the lattice is in an equilibrium state when sampled. The mean energy level μ and standard deviation σ_E are included in the plots, and an additional Gaussian fit is illustrated for comparison in the two $T = 2.4$ cases.

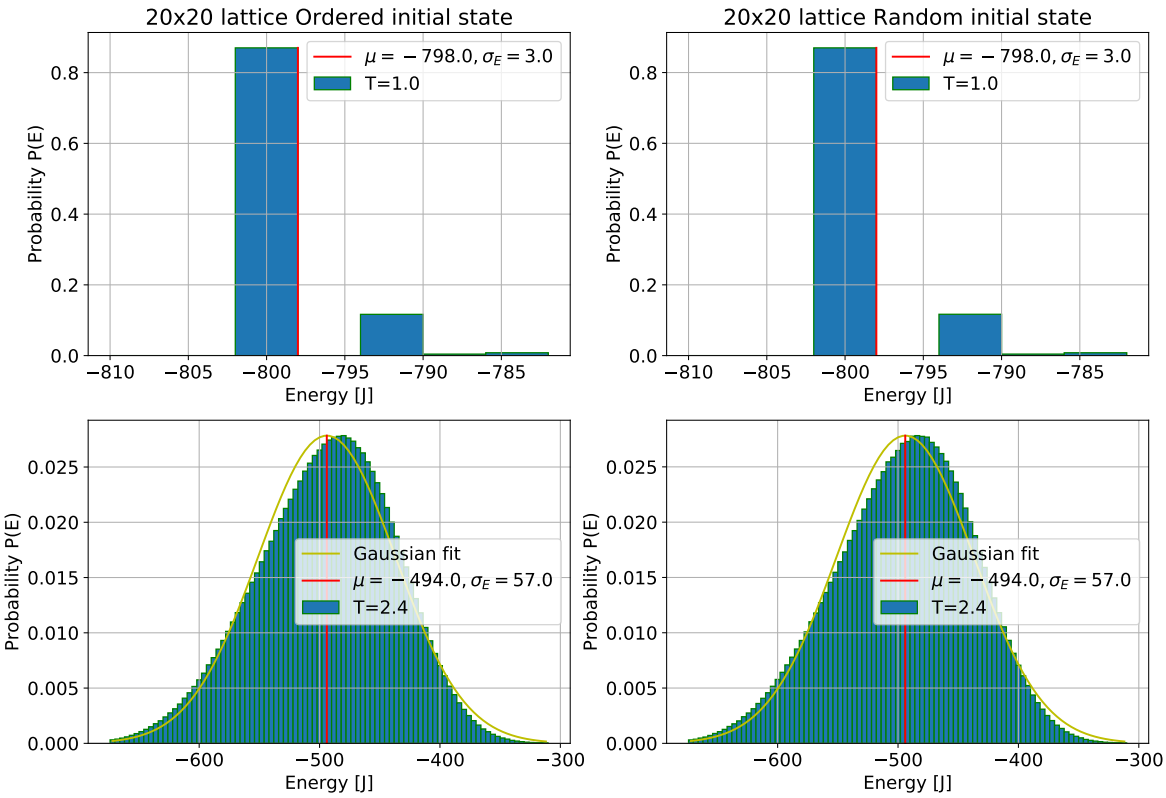

Figure 6: The probability distribution of energy levels counted for the four configurations (ordered, disordered, $T = 1.0$ and $T = 2.4$). All cases involved a 20×20 lattice which was allowed to reach equilibrium by $3 \cdot 10^5$ MC cycles. The rest of the $9.7 \cdot 10^6$ MC cycles recorded the probabilities. The mean and standard deviation was included for each distribution, as well as a Gaussian fit for the distributions of temperature $T = 2.4$.

Phase transition of lattices

Table 4 lists the run-times of the simulation as a function of the CPU's used for several temperatures. These values were obtained from a 40×40 lattice simulation over 10^6 MC cycles with an equilibration time of $S = 4000$.

Simulation run-time for several CPU variants.				
Temperature	1 core $[s]$	2 cores $[s]$	3 cores $[s]$	4 cores $[s]$
2.0	192.13	103.29	88.00	72.51
2.1	193.21	102.25	89.86	72.03
2.2	195.18	101.43	86.55	72.45
2.3	197.26	105.45	93.79	73.19
2.4	200.17	105.06	82.90	72.50
Total	977.95	517.48	441.11	362.68
Average	195.59	103.50	88.22	72.54

Table 4: Run-times of the simulation as a function of the number of CPU's. Several temperatures were included in the temperature vector. The simulation used an equilibrium time of $S = 4000$ and 10^6 MC cycles. The lattice size was 40×40 and was initiated randomly.

Figure 7 illustrates the mean energy per spin, mean magnetization per spin, heat capacity C_V and magnetic susceptibility χ calculated in a large temperature domain. The temperature resolution is set to increase around the critical temperature. Several lattice simulations with varying sizes L are included. Each data point represents a simulation of 10^6 MC cycles with an equilibration time corresponding to the size $S = 250 \cdot L$.

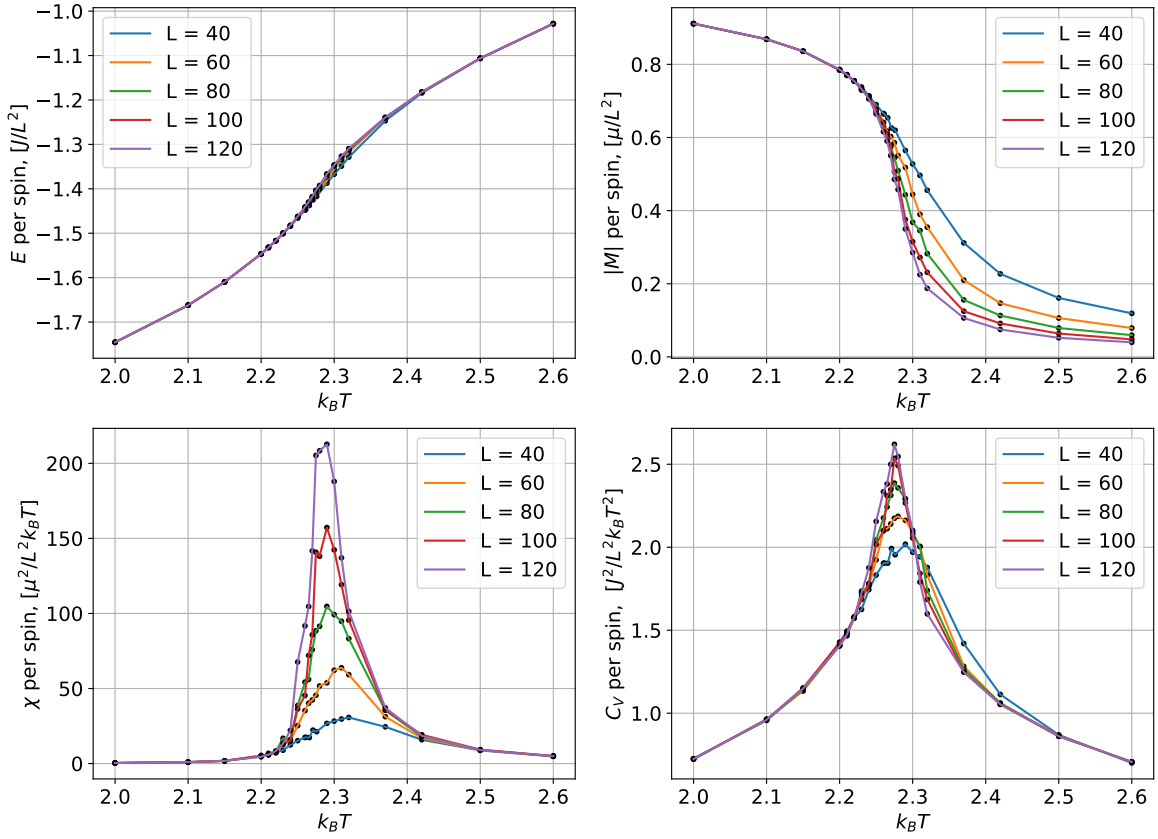

Figure 7: Illustration of the four plots describing the mean energies-, net magnetizations-, heat capacities- and magnetic susceptibilities per spin for several different temperatures. The temperatures go into greater detail around the $T = 2.269$ domain. The lattice sizes simulated are all included in the plots.

Table 5 lists the critical temperatures $T_{C,CV}$ and $T_{C,\chi}$ found by the maximum C_V and χ points for varying lattice sizes L from their plots in figure 7 respectively.

Length L	40	60	80	100	120
$T_{C,CV}$	2.290	2.280	2.280	2.280	2.275
$T_{C,\chi}$	2.320	2.310	2.290	2.290	2.290

Table 5: Table listing all the temperatures which produced maximum points of the heat capacity C_V and magnetic susceptibility χ. The maximum points can be seen in their corresponding graphs illustrated in figure 7. The maximum point temperatures signify the critical temperatures for the given lattice sizes.

Table 6 lists the numerical critical temperature calculations in the thermodynamic limit for all L_1 and L_2 combinations. Both critical temperatures $T_{C,C_V}(L=\infty)$ and $T_{C,\chi}(L=\infty)$ are calculated along with their corresponding mean and standard deviation value. Equation 34 was used for these calculations and the critical temperature values $T_{C,CV}$ and $T_{C,\chi}$ used were listed in table 5.

L_1	L_2	$T_{C,C_V}(L=\infty)$	$T_{C,\chi}(L=\infty)$
40	60	2.260	2.290
40	80	2.260	2.260
40	100	2.265	2.270
40	120	2.268	2.275
60	80	2.260	2.230
60	100	2.268	2.260
60	120	2.270	2.270
80	100	2.275	2.290
80	120	2.275	2.290
100	120	2.275	2.290
Average		2.267 ± 0.006	2.272 ± 0.018

Table 6: Table listing the critical temperatures in the thermodynamic limit $T_C(L=\infty)$ given by the maximum point temperatures listed in table 5. The critical temperature $T_C(L=\infty)$ is calculated using equation 34. All combinations of the lattice sizes L are included. The critical temperature $T_C(L=\infty)$ was calculated by way of C_V and χ independent of each other.

DISCUSSION

Two by two lattice

The behaviour of the simulated lattice is shown to be in good agreement with the analytic expressions by table 2. These results affirm that the programmed simulation model is applicable to the two by two lattice, meaning that it is likely to be reliable for larger lattice simulations as well. While the results have excellent relative error margins, none of which surpass 0.655%, the run-time of the 10-simulation average was $37.2s$ total. This is quite a long run-time for such a small lattice, so the results produced by 10^7 MC cycle simulation are compared for other MC cycle run-times. Table 3 lists these comparisons, illustrating the relative errors of the expectation values $\langle E\rangle$, $\langle E^2\rangle$, $\langle |M|\rangle$ and $\langle M^2\rangle$ as a function of the number of MC cycles. The first few MC cycles such as 10 are quite irrelevant, though the relative errors are quick to decrease below 0.34% after only 10^3 MC cycles.

The weakest calculation results, as visible in table 3, are the numerical heat capacity C_V and magnetic susceptibility χ calculations. Both parameters exhibited relative errors nearly three orders of magnitude larger

than their corresponding expectation values $\langle E \rangle$, $\langle E^2 \rangle$, $\langle |M| \rangle$ and $\langle M^2 \rangle$. This is likely due to the heat capacity and magnetic susceptibility relations with the Helmholtz' free energy F described in the **Theory** section and more specifically by the text following equation 27. The numerical errors of the energy and magnetization are inherited by the heat capacity and magnetic susceptibility respectively due to C_V and χ being the second derivatives of the Helmholtz' free energy.

The candidate which produced the best balanced numerical run-time with sufficient accuracy was that of the 10^5 MC cycle simulation. It's largest error was that of heat capacity (relative error of only 1.7%), and its smallest was that of the mean magnetization $\langle |M| \rangle$ at an impressive relative error of 0.008‰. The calculation time of these parameters was only about $3.72ms$ (based on the 10-time average result taking $37.2ms$). Additionally, the mean magnetization of 10^5 MC cycles turned out to be more accurate than that of the 10^7 MC cycle simulation. This is surprising as the relative error of the results are expected to exhibit a consistent decrease for a larger amount of MC cycles. Nevertheless, this certainly affirms the 10^5 MC cycle simulation as the most reliable for the 2×2 lattice.

Equilibrium time of larger lattice

The behaviour of the 20×20 lattice is fascinating in multiple senses; the research of the equilibrium time was performed and behaved quite oddly, as is illustrated in figure 1. A very large number of randomly initialized lattices reach equilibrium (for $T = 1.0$) relatively early - most of which only take between 50 to 100 MC cycles. The frequency of larger equilibrium times is however quite prominent despite the large spike at the beginning. The distribution decreases quite consistently past 100 MC cycles, though does not reach zero until much later. This is illustrated by figure 2, where there are a surprisingly large amount of lattices which have taken a **far** longer time to reach equilibrium - even up to 2700 MC cycles, there are still multiple initial lattice configurations which have not yet equilibrated. It is unsure what causes this, though it seems that it is quite common.

One of these cases are illustrated by the plots included in figure 3, as the seed chosen for the randomly initiated lattice plots was one which produced an unusually long equilibrium time. For temperatures $T = 1.0$, the ordered initial state energy and magnetization behave as expected, as the ordered state is equivalent with equilibrium (all spins up or down produce an energy minimum). For the disordered initial state, however, the energy level per spin is initialized around 0, and has a sharp decline towards $E = -1.75J$. The lattice stays in this state for almost 3000 MC cycles; it seems to have found some form of unstable temporary preferred state. The magnetization per spin plot is quite chaotic in this time frame, as the system could either equilibrate to all spins pointing up or down and has yet to determine which is preferable. It seems however that once the magnetization per spin reaches approximately +0.5, the rest of the lattice follows and the lattice quickly

transitions to its equilibrium state at $E = -2J$ and $M = +1$. There is reason to believe that this type of temporary preferred state at $-1.75J$ per spin (and perhaps other energy states) is the root cause of some lattices taking so long to reach equilibrium (such as the ones illustrated in figure 2). This can be explained by different regions of the lattice to reaching equilibrium independently, having conflicting steady state spin directions ± 1. The lattice can then oscillate between the two for quite some time before deciding on one preferred orientation. This would require further analysis to be determined.

The system behaves far more chaotically for the temperature $T = 2.4$. The energies of both the ordered and disordered initial state lattices seem to oscillate around $-1.2J$ per spin in both cases, but the variance is far larger than before. The same applies to the magnetization per spin of the two initial states (ordered and random); though the absolute value of the magnetization is illustrated above, both cases were found to oscillate chaotically around all possible configurations between -0.9 and $+0.9$ magnetization per spin. The magnetization of the system seems to have no preferred state but certainly avoids the ferromagnetic orientations of ± 1, as the system now exhibits paramagnetic behaviour.

This behaviour can be characterized by a power rivalry between the energy and entropy. The entropy dictates that the system should reach the most likely state, while energy of the system receives constant contributions from the temperature. The energy would like to minimize to the lowest possible state, namely $-2J$ per spin, though the entropy would always like to increase to a state with larger multiplicity. Seeing as there is are only two configurations (all spins up or down) which produce the state $-2J$ per spin, there are definitively far more states (larger multiplicity) which produce the energy $-1.2J$ per spin which the entropy would rather persist in. While the equilibrium times for $T = 1.0$ are found by observing the MC cycles required for the energy per spin to reach -2.0, there is no clear way of estimating an equilibrium time from the chaotic behaviour observed for $T = 2.4$. This being said, the equilibrium state is likely reached faster for larger temperatures (this certainly is the case for the random initial state, $T = 2.4$ energy graph from figure 3), as the number of accepted configurations is increased.

The difference between the two temperatures is of course reminiscent of the different behaviours of ferromagnetic and paramagnetic materials. This indicates that the critical temperature of the 20×20 lattice is included somewhere between the two temperature cases, $T_C(L = 20) \in [1.0, 2.4]$. It is likely not close to the temperature $T = 1.0$, as the state seems quite stable; for larger temperatures under the critical temperature, the energy remains in equilibrium at $-2J$ per spin, but the magnetization has the ability to spontaneously flip from $+1$ per spin to -1 per spin. This characteristic is not illustrated in the figures but seems to happen more as the temperature approaches the critical temperature T_C, changing from a stable equilibrium state to chaotic energy fluctuations in the limit $T \to T_C$.

The number of accepted configurations analyses also reveal a number of characteristic behaviours of the system. Figure 4 illustrates the total number of accepted configurations as a function of the MC cycles. This data has a direct correlation with the simulation conducted of the random initial state, $T = 1.0$ lattice simulation illustrated in figure 3. That system reaches a temporary preferred state before switching to equilibrium around 3000 MC cycles, as stated previously. The number of accepted configurations data from this simulation also reveals the transition to the equilibrium state; after about 3000 MC cycles, the previous linearly increasing total number of accepted configurations exhibits a switch to a new linear increase with a lesser slope. This spontaneous slope decrease occurs at the same time as the equilibrium state $-2J$ per spin is reached in the corresponding energy graph (the same RNG seed was used as the random initial state, $T = 1.0$ energy plot from figure 3). This is due to the number of accepted configurations in a non-equilibrium state being far larger than the equilibrium state, as partially shown by the fluctuations in magnetization (random initial state, $T = 1.0$ from figure 3). Since the magnetization represents the sum of all the up- and down spins, the fluctuations can reveal the number of spins flipped (how many configurations are accepted) for each MC cycle. This degree of fluctuation in magnetization is clearly larger prior to the equilibrium state, as is also revealed by the slope change of the curve from figure 4.

The number of accepted configurations as a function of temperature illustrated by figure 5 behaves quite interestingly, as it seems to increase proportionally to e^x up to a certain point. This is consistent with the condition presented in equation 38, which states that a larger temperature causes more states to be accepted. Increasing the temperature causes the exponential to decrease due to the definition $\beta = 1/(k_B T)$, such that the same energy changes ΔE have a larger probability (compared to smaller temperatures) of being accepted. The figure increases exponentially up to a point around $T \approx 2.37$ (read by-eye), where the number of accepted states slope begins to decline. This seems to be caused by the critical temperature transition, where the number of accepted states now increases by a decreasing slope (similar to the function $e^{-1/x}$). The number of accepted states after the critical temperature proceeds to increase towards an upper boundary, namely 1. One accepted state per spin is equivalent to L^2 spin flips for an $L \times L$ lattice, signifying that every spin is flipped on average. This is the case for the lattice in the temperature limit $T \to \infty$, as the exponential $-\Delta E/kT \to 0$ for any ΔE. This means that the acceptance condition described in equation 38 is always fulfilled.

Energy distribution analysis

The energy distribution plots from figure 6 illustrate the characteristic difference between the two temperatures $T = 1.0$ and $T = 2.4$, namely the energies degree of fluctuation around the mean. The $T = 1.0$ graphs are quite intuitive: The lattice reaches a steady state at total energy $-800J$ (analogous to $-2J$ per spin) and rarely fluctuates to the neighboring energies. The energy level $-792J$ is the second most probable at about 10%

occurrence probability; this state is reached by a single electron flip, as the change in energy with its neighbors goes from being $-4J$ to $+4J$ (total $\Delta E = +8J$). As for the probability for an energy -796, there are in fact no configurations of the lattice which produce the state. The probability of finding this energy level is therefore zero, as is consistent with the plots.

The degree of fluctuation around the mean for the $T = 2.4$ plot is far greater, as is illustrated by the corresponding graphs in figure 6. Though the $T = 1.0$ graphs have no Gaussian resemblance (due to the energy only fluctuating in one direction), the $T = 2.4$ graphs greatly resemble Gaussian distributions. To see if this matched, a Gaussian fit was implemented using the calculated means μ and standard deviations σ_E listed in the plot legend. This implementation turned out to reveal something fundamental about the distribution, as it's gradual increase and sharp decrease are reminiscent of a Maxwell-Boltzmann energy distribution. This is strange as Maxwell-Boltzmann distributions typically have a sharper increase for lower energies and a more gradual decrease to higher energies, the opposite of what is observed of the 20×20 lattice. This will not be gone into greater detail since it is not the main focus of the research, though an additional analysis of this distribution is tempting.

There seems to be no difference in the energy distribution comparison between the initially ordered and initially disordered lattice variants. This indicates that the lattice is not influenced by its previous configurations in any sense; if the lattice has reached equilibrium it will behave as if it were initialized as such, and evolves accordingly. This seems to be the case for temperatures below and above the critical temperature T_C, as is illustrated in the plots.

Phase transition of lattices

The simulation run-time was successfully optimized through the parallelization of many CPU's. The degree of optimization produced by adding multiple CPU's is illustrated by table 4, revealing some interesting behaviour behind the MPI package's CPU job division. Since each core was assigned its own spectrum of MC cycles, there should be no systematic lag where one core completes it's job before another. This lag could occur if the division assigned different temperatures to different cores. This is due the fact that a larger temperature T results in a larger number of accepted configurations (meaning more floating point operations) as illustrated by figure 5 and discussed previously. This calculation time increase (due to a larger number of floating point operations) is well illustrated by the run-times using just one core. It increases quite regularly by increments of about 2 seconds for increasing temperatures. This phenomena is however for some reason more difficult to identify for more cores.

The average simulation time nearly halved (went from 195.59s to 103.50s) by changing from one core to two, a decrease in run-time of about 53%. This effect was however not as noticeable when doubling the cores once more. The time difference from two cores to four was 103.50s to 72.54s, only a relative decrease by about 70%. It is worth noting that the time decrease from tripling the cores (from one to three) decreased the run-time by about 45%, while it ought to be closer to 33%. These are interesting computational results as they illustrate an inconsistency of the experimental equipment used, namely the computer conducting the simulation. The results listed in table 4 are characteristic to several situational specifications (hardware, software, environment, etc.) which can cause run-time fluctuations. The computer's conditions were not accounted for although it seems to have had a larger impact for an increasing number CPUs called upon. The four CPU calculation times do for example **not** illustrate the systematic increase in run-time (due to floating point operations) as the one CPU run-times do, indicating some computational run-time fluctuations as the cause.

Figure 7 illustrates the final E/L^2, $|M|/L^2$, C_V/L^2 and χ/L^2 results of several exhaustive calculations. An additional lattice size $L = 120$ was included for more detailed C_V and χ extremum points. The calculation run-time for this lattice size was in the 5 hour mark, so the current results are regarded as sufficient for critical temperature extraction. Larger lattices or more detailed temperature scales would undoubtedly produce more reliable data, though the severe run-times are not justifiable by slightly more accurate results.

As for the data illustrated, there are excellent visual discontinuities to be seen in both the heat capacity and magnetic susceptibility plots. The heat capacity has a more exaggerated discontinuity spike for larger lattices, while the magnetic susceptibility had a vaguer maximum point, illustrating three similar data points at the top of the 120×120 curve. As for the mean energy and magnetization per spin graphs, there is a noticeable decline in magnetization around a temperature around $T = 2.3$, which occurs more spontaneously for larger ordered lattices. This spontaneous demagnetization is likely perfectly vertical for $T \to T_C$ in the thermodynamic limit $L \to \infty$. The mean energy per spin seems to be the parameter least impacted by the critical temperature transition, as it only exhibits a slight increase in slope in the interval $[2.25, 2.30]$ (which is a domain including the theoretical temperature). This is the only irregularity displayed, as the energy increases somewhat linearly prior to- and after this interval.

Table 5 lists the temperatures which produced maximum points for each lattice size $L \in [40, 60, 80, 100, 120]$ for both the C_V and χ data sets. These maximums are meant to symbolize the discontinuity points, although the spike is certainly more prominent for some lattice sizes than others. More specifically, the maximum point of C_V for lattice size $L = 40 \times 40$ is quite vague, whereas the maximum points for larger lattices are far more precisely defined. This is well illustrated by the data in the table, as both T_{C,C_V} and $T_{C,\chi}$ converge towards the critical temperature 2.269 for increasing lattice sizes: T_{C,C_V} transitions from 2.290 to 2.275 and $T_{C,\chi}$ transitions from 2.320 to 2.290.

These maximum points are thereafter utilized in equation 34 to extract the critical temperature in the thermodynamic limit. This is done by using all possible lattice combinations L_1, L_2 and critical temperatures from the previous table. This is done by way of C_V and χ independently to determine the more accurate extraction process. In comparison with the benchmark $T_C = 2.269$, both results have standard deviations (uncertainties) which include T_C in their domain. The most accurate of these, however, is the theoretical $T_{C,C_V}(L = \infty) = 2.267 \pm 0.006$ produced by the heat capacity. This result came just 0.002 off from the benchmark, which was well within the uncertainty. In comparison, the result produced by the magnetic susceptibility $T_{C,\chi}(L = \infty) = 2.272 \pm 0.018$ was very accurate in relation to the benchmark as well, though by a larger uncertainty. This larger uncertainty is due to the inconsistency of the spikes from it's corresponding plot in figure 7. The heat capacity had better defined spikes which produced a more accurate result for lower lattice sizes L. The magnetic susceptibility critical temperature extraction was very successful though, as it was only $0.003 = \sigma_\chi/6$ off.

It is worth noting that the resulting critical temperatures from the lower lattice sizes $L = 40$ and $L = 60$ should perhaps not be held to the same standard as the larger lattices $L = 100$ and $L = 120$. The thermodynamic limit critical temperature was calculated by way of averaging all the lattice combination results, though weights corresponding their accuracies could also be implemented. The larger lattices should carry far more significant results, though this is not the behaviour seen in table 6. The L_1 and L_2 combination which seems to produce the most accurate result is $L_1 = 60 \cup L_2 = 120$. This lattice combination produced the most accurate (in relation to the benchmark $T_C = 2.269$) result for both data sets C_V and χ. There seems to be no specific reasoning behind this as equation 34 has no preferences for the L parameter values, meaning that this can likely be chalked up to a result of probabilities and coincidental occurrences.

CONCLUSION

The simulation of the two by two lattice coincided very well with the analytic results presented. The most efficient simulation time to produce accurate expectation value results was asserted to be 10^5 MC cycles, as it exhibited an excellent compromise between accuracy and numerical precision. The equilibrium times of the 20×20 lattices at temperature $T = 1.0$ were found to be largely centered around 50 MC cycles, though an incredibly large number of lattices took up to 2000 MC cycles to stabilize. This was shown in the energy plot to be due to a semi-steady energy state of $E = -1.75J$ per spin (for one case), which the lattice lingered on for a long time. During this time the magnetization fluctuated back and forth between -1 and $+1$, unsure as to which state is preferable. The number of total accepted configurations as a function of the MC cycles revealed that there are far more configurations accepted in the non-equilibrium state compared to equilibrium. The number of total accepted configurations as a function of the temperature also revealed that the number increased exponentially up to a certain point, where it began to decline more. The probability distribution of the 20×20 lattices revealed that the there is no intrinsic difference in the initialization of a lattice. As long as equilibrium is reached, the macroscopic measurements of the system are characteristic to the size of the lattice, temperature and the coupling model used. The energy distribution of the lattice at temperature $T = 1.0$ was found to be rectified, and $T = 2.4$ was found to be non-Gaussian. The simulation was successfully optimized through parallelization of the code. The largest run-time difference was produced by switching from one core to two, producing a decrease in run-time to about 53% of the original. The parallelized simulation of the lattice produced data adequate for a proper critical temperature extraction. Both temperature extractions of C_V and χ were within the $T_C = 2.269 k T_C J^{-1}$ benchmark of the results. The critical temperature extracted from C_V was found to be the most accurate at $T = 2.267 \pm 0.006 k T_C J^{-1}$.

References

[1] Mikusheva, P. A. (2007). Mcmc: Metropolis hastings algorithm-mit opencourseware.

[2] Morten, H.-J. (2015). Lecture notes fall 2015.

[3] Onsager, L. (1944). Crystal statistics. i. a two-dimensional model with an order-disorder transition. *Phys. Rev.*, 65:117–149.

[4] Press, W. H., Flannery, B. P., Teukolsky, S. A., and Vetterling, W. T. (1992). *Numerical Recipes in Fortran 77: The Art of Scientific Computing*. Cambridge University Press.

[5] Press, W. H. and Teukolsky, S. A. (1992). Portable random number generators. *Computers in Physics*, 6(5):522.

[6] Schroeder, D. (1999). *An Introduction to Thermal Physics*. Addison Wesley.